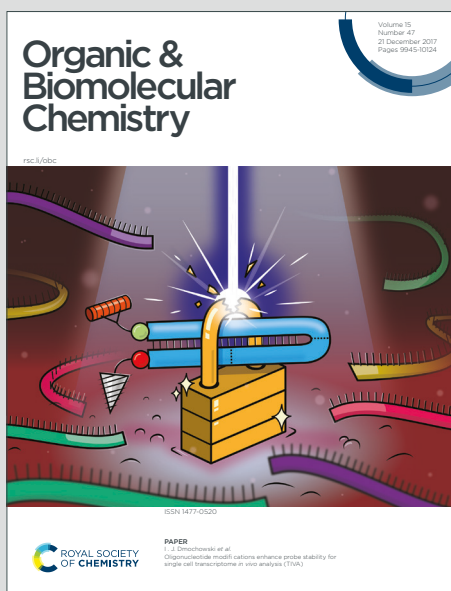


Organic & Biomolecular Chemistry

Accepted Manuscript

This article can be cited before page numbers have been issued, to do this please use: Y. liao, Z. ye, M. Qian, X. wang, Y. guo, G. Han, Y. Song, J. hou and Y. Liu, *Org. Biomol. Chem.*, 2020, DOI: 10.1039/D0OB00564A.



This is an Accepted Manuscript, which has been through the Royal Society of Chemistry peer review process and has been accepted for publication.

Accepted Manuscripts are published online shortly after acceptance, before technical editing, formatting and proof reading. Using this free service, authors can make their results available to the community, in citable form, before we publish the edited article. We will replace this Accepted Manuscript with the edited and formatted Advance Article as soon as it is available.

You can find more information about Accepted Manuscripts in the [Information for Authors](#).

Please note that technical editing may introduce minor changes to the text and/or graphics, which may alter content. The journal's standard [Terms & Conditions](#) and the [Ethical guidelines](#) still apply. In no event shall the Royal Society of Chemistry be held responsible for any errors or omissions in this Accepted Manuscript or any consequences arising from the use of any information it contains.

Photoactive NO hybrids with pseudo-zero-order release kinetics for antimicrobial applications

View Article Online
DOI: 10.1039/D0OB00564A1Received 00th January 20xx,
Accepted 00th January 20xx

DOI: 10.1039/x0xx00000x

Yongfang Liao, Zizhen Ye, Meng Qian, Xing Wang, Yuda Guo, Guifang Han, Yuguang Song, Jingli Hou*, Yangping Liu*

Bacterial infection is a major threat to health and life of human due to development of drug resistance, which is related to biofilm formation. Nitric oxide (NO) has emerged as an important factor in regulating the biofilm formation. In order to harness the potential benefit of NO and develop effective antibacterial agents, we designed and synthesized a new class of NO hybrids in which active scaffold benzothienoazepine was tagged with a nitroso group and further conjugated with quaternary ammoniums or phosphoniums. The temporal release of NO from these hybrids can be achieved by photoactivation. Interestingly, the NO release follows a pseudo-zero-order kinetics, which is easily determined by measurement of the fluorescent benzothienoazepine or NO. Compared to positive control ciprofloxacin, the NO hybrid with triphenyl phosphonium (TPP) exhibited more effective activity against *S. aureus* biofilm in darkness. Irradiation of the NO hybrid led to higher inhibition against *S. aureus* biofilm than the parental NO hybrid in darkness or the corresponding NO-released product, indicating the combined effect of NO and the NO-released product. Therefore, this new class of NO hybrids are very promising antimicrobial agents and this work provides a new way for design of highly effective antimicrobial agents.

Introduction

Bacterial infection is a major threat to the health and life of human from the onset of human existence. It has been estimated that at least of 60% of bacterial infections currently treated by physicians in the developed world are considered to involve biofilm formation.¹ Once established, the biofilms are extremely difficult to eradicate by antimicrobial treatment. Clinically, biofilm infections represent an overwhelming issue, because biofilms usually cause persistent and chronic infections due to drug resistance. Bacteria with biofilms are highly (10-1000 fold) resistant to antimicrobials that are effective in the treatment of these same bacteria in planktonic growth mode.²⁻⁵ However, there is a lack of effective antibiofilm agents to eradicate biofilm-related infections. Therefore, it is of great importance to develop new type of medicines that target bacterial biofilm formation.

The signalling molecule nitric oxide (NO) has emerged as an important factor in regulating biofilm formation.⁶ It was reported that nanomolar concentrations of NO prevent initial biofilm formation and induce a transition from the biofilm to the planktonic mode of growth *via* multiple mechanisms, including cyclic-di-GMP signalling, nitric oxide signalling, quorum sensing and so on.⁶⁻⁹ Moreover, low-dose NO is used as targeted adjunctive therapy to disperse *Pseudomonas aeruginosa* biofilm in cystic fibrosis.¹⁰ Consequently, NO donors such as sodium nitroprusside and nitrofurazone exhibit excellent activity to induce biofilm dispersal.^{5, 11-13}

Furthermore, NO hybrids with combined antibiofilm and antibacterial activities had been developed to kill *Pseudomonas aeruginosa*.¹⁴ Even with the promising results, the therapeutic applications of NO donors are limited since most of them lead to spontaneous generation of NO in aqueous solution. In order to harness the potential benefits of NO, it is extremely desirable to liberate NO at the local site with precise concentration and specific duration. Photo-induced NO donors are potential candidates to meet the needs since they allow the release of NO in a precise spatial and temporal mode by controlling the site, duration and intensity of the light.

Various types of photo-induced NO donors have been developed, such as metal nitrosyls,¹⁵ nitrobenzene¹⁶ and *N*-nitroso-amines,¹⁷⁻¹⁹ which enable the NO release in a precise spatial and temporal mode by controlling of the site, duration and light intensity. Although significant progress has been achieved in the development of photo-induced NO donors, some challenges still remain. Particularly, the donors usually release NO in a "fast-then-slow" manner, leading to the fluctuation of NO concentrations. Since the therapeutic consequence of NO-based drugs depends strongly on the concentrations of NO delivered, effective NO-based therapies should only deliver desirable NO doses. In this context, the NO donors with constant release rates during the entire release process are very appealing.

Considering that aromatic amine is an important moiety in bioactive molecules, we focused on *N*-aryl-nitrosamines to design a novel NO hybrid with high atom economy, which can undergo homolytic cleavage of N-NO bond upon irradiation to give NO and the corresponding aromatic amine derivative.²⁰ Similar strategy was used to design near-infrared photoactivatable NO donors which enabled integrated photoacoustic monitoring.¹⁸ In order to develop antimicrobial-based photoactivatable NO hybrids, an aromatic amine-

Tianjin Key Laboratory on Technologies Enabling Development of Clinical Therapeutics and Diagnostics, School of Pharmacy, Tianjin Medical University, Tianjin 300070, P. R. China. E-mail: liuyangping@tmu.edu.cn; houjingli@tmu.edu.cn

Electronic Supplementary Information (ESI) available: See DOI:10.1039/x0xx00000x

containing antimicrobial is desirable for the attachment of nitroso group. Benzothienoazepine derivatives had been reported as respiratory syncytial virus inhibitors.²¹ In the initial screening, its derivatives (ester form) displayed weak activity against Gram-positive bacteria *S. aureus* (Fig. S10), thus Benzothienoazepine was selected as an antimicrobial (Fig. 1). In addition, its fluorescence properties are also appealing because NO release can be monitored by fluorescence method. To enhance the antimicrobial activity, the benzothienoazepine was conjugated with quaternary ammonium or phosphonium compounds (QACs or QPCs) that target bacterial cytoplasm and caused the loss of the structural organization and integrity.²² These QACs and QPCs have been widely used to prepare antibacterial materials due to their potent and broad-spectrum activities.²³ The final photoactivatable NO hybrids were then constructed by *N*-nitrosation on the QACs/QPCs-conjugated benzothienoazepine core (Figure 1). In this work we demonstrated that this type of NO hybrids could achieve NO steady release by light at a zero-order rate, evidenced by the yielded fluorescent product and NO generation. In contrast to the commonly used antibiotic drug ciprofloxacin, these hybrids showed potent effects against *S. aureus* biofilm.

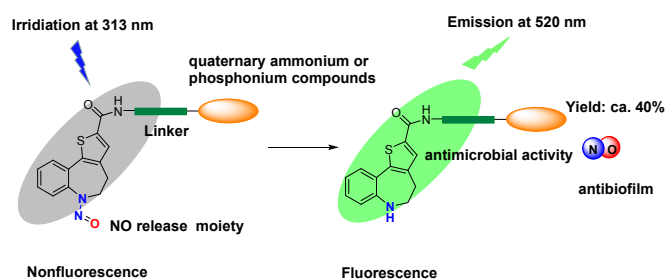


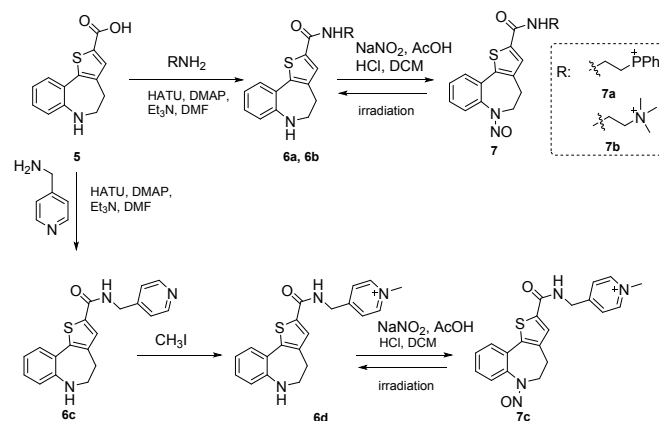
Figure 1. Design of light-induced NO hybrids from benzothienoazepine core and quaternary ammonium/phosphonium moieties to kill or inhibit bacterial biofilm.

Results and discussion

Synthesis and characterization of NO hybrids

The key intermediate benzothienoazepine (**5**) was obtained *via* 4 steps with a total yield of 50% from commercial 1,2,3,4-tetrahydro-benzo[*b*]azepin-5-one (**1**) according to the previously reported procedure (see S1).²⁴ Interestingly, the benzothienoazepine (**5**) has a strong fluorescence emission at 500 nm which has not been revealed since its initial synthesis in 1993 (Fig. S1). The fluorescence quantum yield of **5** was determined to be 0.79 in ethanol (Fig. S2) and a large Stokes shift (130 nm) was observed with excitation/emission maxima at 370/500 nm in phosphate buffered saline (PBS). Thus, the compound **5** can be potentially used to develop photo-calibrated NO donors which allow conveniently monitoring of NO release in a real-time mode by fluorescence method.^{19, 25}

To study the antibacterial effect of the cationic groups, triphenyl phosphonium (TPP), trimethyl ammonium and pyridinium groups were chosen. The cationic groups TPP and trimethyl ammonium were directly connected to compound **5** *via* amide coupling reaction, followed by *N*-nitrosation of the secondary amine to afford the corresponding NO hybrids (**7a** and **7b**, Scheme 1). The other NO hybrid bearing pyridinium (**7c**) was obtained by linkage of the pyridine group to the compound **5**, followed by sequential *N*-methylation of the pyridine and *N*-nitrosation. The target compounds (NO hybrids) were characterized by ¹H NMR, ¹³C NMR and HRMS. HPLC analysis indicated good purity (>95%) and excellent stability of these NO hybrids without observable decay in CH₃CN in the dark for 24 h (Fig. S3-4).



Scheme 1. The synthetic routes of the NO hybrids.

Photo-response of NO hybrids

To investigate the photo-response of **7a-c**, the UV-vis absorption spectra of each compound (40 μM) in PBS (20 mM, pH = 7.4, containing 5% DMSO) were recorded intermittently during irradiation. The maximum absorption of **7a** is located at 313 nm with a molar absorption of 17650 cm⁻¹ M⁻¹. Upon irradiation **7a** with UV light (313 ± 10 nm, 6 W LED light) in quartz cuvette, the absorption of **7a** at 313 nm was weakened, accompanied with the increase in the absorption of **6a** at 365 nm. A linear relationship between the concentration of **6a** and time was observed upon irradiation (Fig. 2a), indicating that the photo-induced denitrosation of **7a** follows pseudo-zero-order kinetics. The denitrosation rate of **7a** was determined to 0.24 μM min⁻¹. Similarly, the photo-triggered denitrosation of **7b** and **7c** were also observed with irradiation at 313 nm and followed pseudo-zero-order decomposition kinetics, with the rates of 0.18 μM min⁻¹ for **7b** and 0.23 μM min⁻¹ for **7c**, respectively (Fig. 2b, c). Therefore, it can be concluded that the three NO hybrids have the similar photo-triggered denitrosation rates, and the cationic group has little effect on their denitrosation.

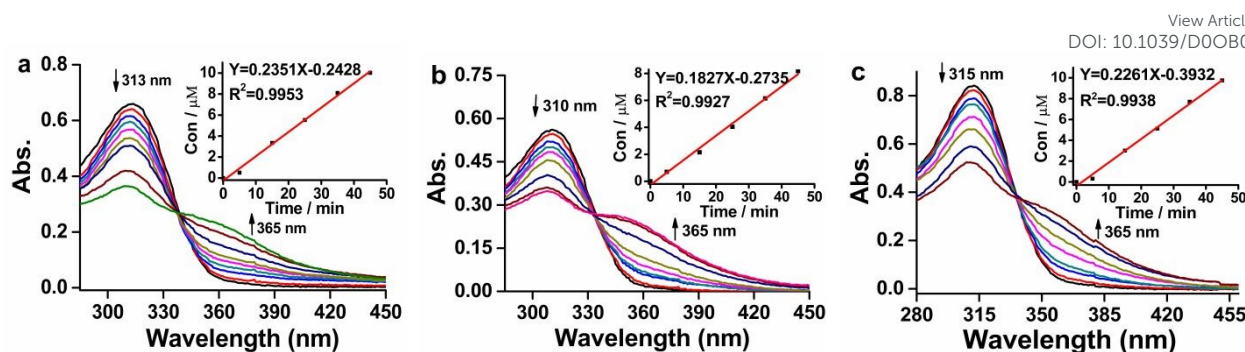


Figure 2. (a, b, c): The time course changes of UV-vis absorption of **7a**, **7b** and **7c** solution (40 μM) upon irradiation by light 313 nm; Inset: The dynamic relationship between the concentrations of product (**6a-b** and **6d**) and exposure time to irradiation by fitting the absorption at 365 nm, respectively.

To check if the photo-triggered denitrosation of **7a-c** can be monitored by fluorescent spectroscopy, we first measured the fluorescent spectra of the NO hybrids (**7a-c**) as well as their precursors (**6a-b** and **6d**). All the NO hybrids are essentially non-fluorescent with the fluorescence quantum yields (Φ) of 0.0022, 0.0033 and 0.0013 for **7a**, **7b** and **7c**, respectively (Fig. S2), while the precursors, except for **6d**, show strong fluorescence emission at around 520 nm. The quantum yields were estimated to be 0.557 and 0.564 for **6a** and **6b** in ethanol, respectively. The tremendous difference in fluorescent intensities of the NO hybrids and precursors suggests that the denitrosation reaction of the hybrids can be monitored by fluorescence method. Subsequently, we investigated the

fluorescent stabilities of the hybrids (**7a-b**) and their precursors (**6a-b**) to ensure the detective reliability. As indicated in Fig. 3, only negligible changes in fluorescence intensity were observed for hybrids (**7a-b**) and precursors (**6a-b**) in the presence of different pH buffer (5.0-8.0), various cations (K^+ , Na^+ and Zn^{2+}), and amino acids, such as arginine (Arg), cystein (Cys) and glutathione (GSH) and so on. The results indicated there are no unexpected fluorescence changes from hybrids and NO-released products. The above properties ensured the reliability of fluorescence based calibration method to monitor the denitrosation reaction of NO hybrids.

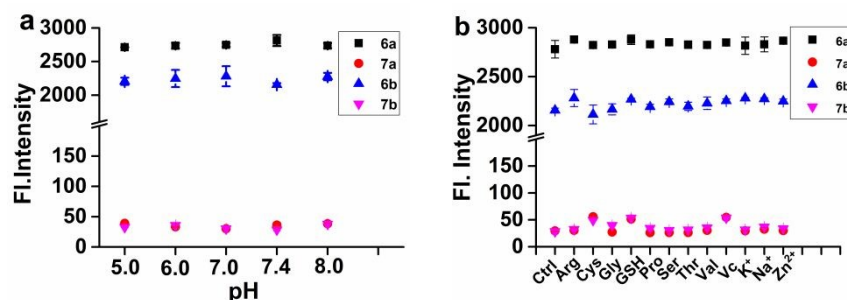


Figure 3. The fluorescence stability of NO hybrids and their precursors. (a) pH effect on fluorescence intensity; (b) fluorescence interference from amino acids and cations. The NO hybrids and their precursors were prepared at the concentration of 5 μM . $\lambda_{\text{ex}} = 375 \text{ nm}$, $\lambda_{\text{em}} = 520 \text{ nm}$, slit = 5 nm/5 nm.

As shown in Fig. 4a, the fluorescence intensities in the solution of **7a** (5 μM) increased in a time-dependent manner upon irradiation at 313 nm. To confirm the generation of **6a** from the denitrosation reaction of **7a**, the reaction mixture was subjected to HPLC analysis. In addition to the peak of **7a** at 10.11 min, a new peak appeared at 6.01 min in the reaction mixture, which is the same as that of the authentic **6a** (Fig. S5). The generation of **6a** from the denitrosation reaction of **7a** was further verified by high resolution mass spectrometry (HRMS) studies (Fig. S5). In addition, a good linear relationship was observed between the fluorescent intensities of **6a** and its concentrations in the range of 0 ~ 5 μM (Fig. S6). Based on this relationship, the concentration of **6a** generated from **7a** upon irradiation was conveniently calculated. The results showed

that the photo-triggered generation of **6a** from **7a** was linearly correlated with time and the rate of the pseudo-zero-order kinetics was calculated to be 0.23 $\mu\text{M min}^{-1}$ (Fig. 4a), in good agreement with the value obtained by UV-vis absorption method. Moreover, we also plotted the fluorescence intensity changes for **7b** as a function of the irradiation time and the generation rate of **6b** was calculated to be 0.21 $\mu\text{M min}^{-1}$ (Fig. 4b). Due to the weak fluorescence of **6d** (Fig. S7), its generation rate from **7c** could not be obtained using the fluorescence method. Taken together, the photo-triggered denitrosation reactions of **7a** and **7b** can be also monitored by fluorescence method, indicating that NO release could be convenient detected by the fluorescence increase.

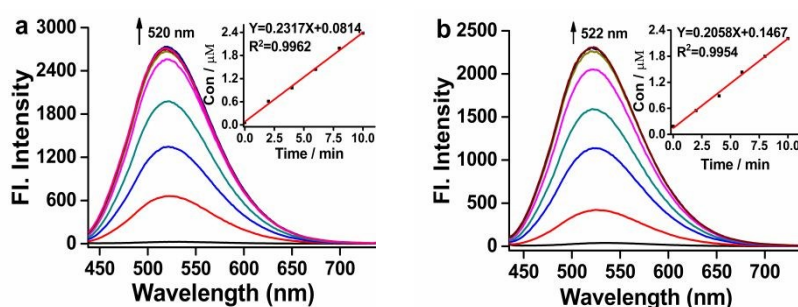


Figure 4. The time course changes of fluorescent spectra of **7a** (a) and **7b** (b) solutions ($5 \mu\text{M}$) by light irradiation; $\lambda_{\text{ex}} = 375 \text{ nm}$, $\lambda_{\text{em}} = 520 \text{ nm}$, slit = $5 \text{ nm}/5 \text{ nm}$. Inset: The linear relationship between the concentrations of the product (**6a** or **6b**) and irradiation time.

NO release from NO hybrids

To confirm NO release from the photo-induced denitrosation of **7a**, the EPR spin trapping reagents *N*-methyl-*D*-glucamine dithiocarbamate-iron (II) Fe^{2+} -(MGD)₂ was employed. MGD-Fe traps NO efficiently to form NO-Fe-MGD complex, which has a typical triplet signal with a nitrogen hyperfine coupling constant (a_{N}) between 12.5–13.2 G. All the samples were subjected to irradiation in a quartz EPR tube. As shown in Fig. 5a, the typical signal was not observed in the dark after addition of **7a** ($40 \mu\text{M}$) to the Fe^{2+} -(MGD)₂ solution. Upon irradiation, a typical triplet signal ($a_{\text{N}} = 12.95 \text{ G}$) for NO-Fe-MGD complex appeared and increased with the irradiation time, indicating that substantial amount of NO was produced from **7a**. Moreover, the photo-induced generation of NO-Fe-MGD from **7a** increased linearly in 0.5 h and then reached a plateau. The time course of EPR signal intensities showed a pseudo-zero-order kinetics for the NO generation with the rate of $1.20 \mu\text{M min}^{-1}$. Note: the rate is much higher than the values (0.23 – $0.24 \mu\text{M min}^{-1}$) obtained by UV-vis and fluorescence

methods due to the different irradiation condition used: **7a** solution was irradiated in quartz EPR tube (1.0 mm , id) for EPR experiments, but in 1-cm quartz cuvette for UV-vis and fluorescent experiments. The NO release rates for **7b** and **7c** was similar to that of **7a**, with the value as 1.40 and $1.25 \mu\text{M min}^{-1}$ respectively (Fig. S8). It was worth mentioning that the zero-order kinetics ensured constant release of NO unlike the previous NO donors with one-order kinetics^{26, 27}. The accumulative concentration of NO released from **7a** ($40 \mu\text{M}$) was calculated to be about $17.2 \mu\text{M}$, based on TEMPO standard curve.²⁸ The yield of NO from **7a** was about 43%. This result was further confirmed by the Griess method in which nitrite (NO_2^-), the final product of NO in air, was measured.²⁹ The yield of NO_2^- formation was about 38%, 37% and 38% by Griess method for **7a**, **7b** and **7c** respectively (Fig. S8). These results support that NO is released from these NO hybrids by light irradiation.

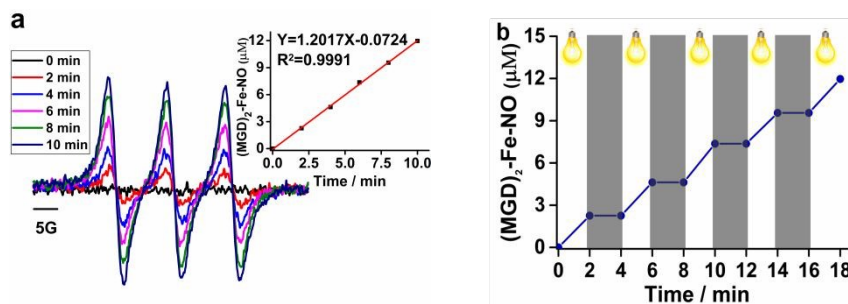


Figure 5. (a) The EPR spectra of [(MGD)₂-Fe-NO] in the presence of **7a** ($40 \mu\text{M}$) with or without irradiation at 313 nm ; EPR spectra were recorded after photo-irradiation for 0, 2, 4, 6, 8 and 10 min with a modulation frequency of 100 KHz, a modulation amplitude of 1 G and a microwave power of 10 mW; inset: the relationship between NO generation and irradiation time; (b) NO-capture curve of **7a** under 313 nm light irradiation for different on/off cycles. Samples contained 5 mM of MGD and 1 mM of $(\text{NH}_4)_2\text{Fe}(\text{SO}_4)_2$.

Next, we examined whether NO release from **7a** could be controlled with temporal precision by light irradiation. A buffered solution containing **7a** and Fe^{2+} -(MGD)₂ was exposed to the triggering light (313 nm). As shown in Fig. 5b, the EPR signal for the NO adduct [(MGD)₂-Fe-NO] increased immediately upon irradiation, while the signal remained unchanged when

the irradiation was stopped. The re-irradiation by light led to the increase of the EPR signal again. Similar results were also observed in **7b** and **7c** (Fig. S9). The “on/off” feature of the photo-triggered NO generation indicated that temporally precise manipulation of NO release from these NO hybrids can be achieved.

Antibacterial activities of the NO hybrids

Subsequently, we tested the antibacterial activities of the NO hybrids and their precursors against planktonic bacteria. Positive-gram bacteria *S. aureus* ATCC12600^{GFP} was selected which is sensitive to cationic disinfectants. Minimum inhibitory (MIC) and bactericidal (MBC) concentrations were detected to evaluate the antibacterial activity of the NO hybrids and their precursors. The results indicated that the TPP-bearing hybrids **7a** and its NO precursor **6a** exhibited superior antibacterial

activities than the hybrids with quaternary ammoniums (**6b**, **6d**, and **7b-c**), evidenced by the remarkable reduced OD_{600nm} and the lower MIC (ca. 30 µg/mL) and MBC (ca. 60 µg/mL) value (Fig.6 and Table S1). It was consistent with the previous report that phosphonium-bearing polymers showed better antibacterial activity than the polymers containing the quaternary ammonium salt.^{22, 30, 31}

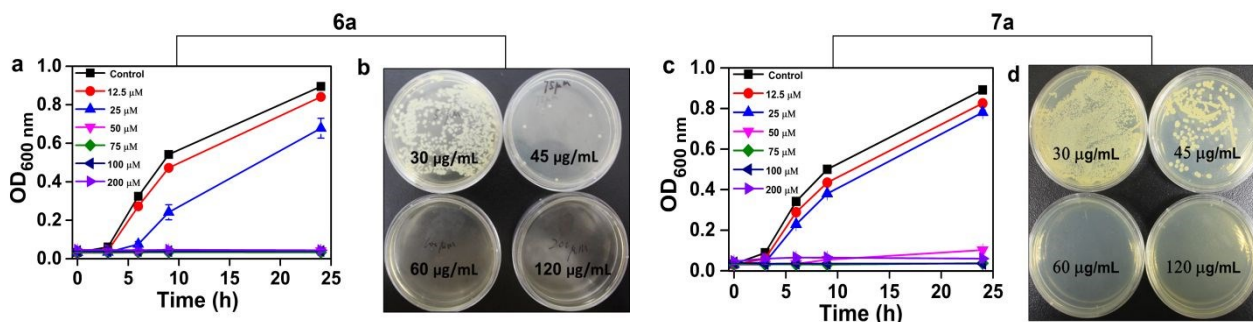


Figure 6. (a, c) Optical density measurements for *S. aureus* ATCC12600^{GFP} in the presence of different concentrations of **6a** and **7a** (7.5-120 µg/mL). The error bars represent the standard deviations of three independent measurements. (b, d) Pictures of Agar plated solutions (30, 45, 60 and 120 µg/mL) which were used to determine the minimum bactericidal concentrations (MBC) after 24-h treatment in the dark. MBC was determined by agar dilution method as being the lowest concentration of drug to kill 99.9% of bacteria which produce no colonies on the plate.

The biofilm formation of *S. aureus* protects the bacterium against antibiotic assault and enhances its recalcitrance.^{32, 33} Therefore, we tested the antimicrobial efficacy of the most potent compounds **7a** and **6a** against *S. aureus* biofilm. After 48-h growth, *S. aureus* biofilm was exposed to **7a**, **6a** or antibiotic drug ciprofloxacin at 37°C. Fig. 7 showed the viable cell counts in the biofilm after treatment with **6a**, **7a** and ciprofloxacin for different times. Clearly, both **7a** and **6a** were very effective against biofilm cells and showed the similar efficacy. 4-log colony forming units (CFUs) were reduced after

treatment with **7a** or **6a** at the concentration of 60 µg/mL for 8 h, while only 2-log reduction in the CFUs count was observed for ciprofloxacin at the concentration of 100 µg/mL after incubation for 8 h (Fig. S11). Although only a slight reduction in CFUs count was detected at lower concentration (30 and 45 µg/mL), increasing the concentration (120 or 180 µg/mL) led to further reduction of the CFUs count (more than 6-log). At 24 h, the effect became weaker, and 2-log reduction in CFUs was detected at the concentration of 60 µg/mL.

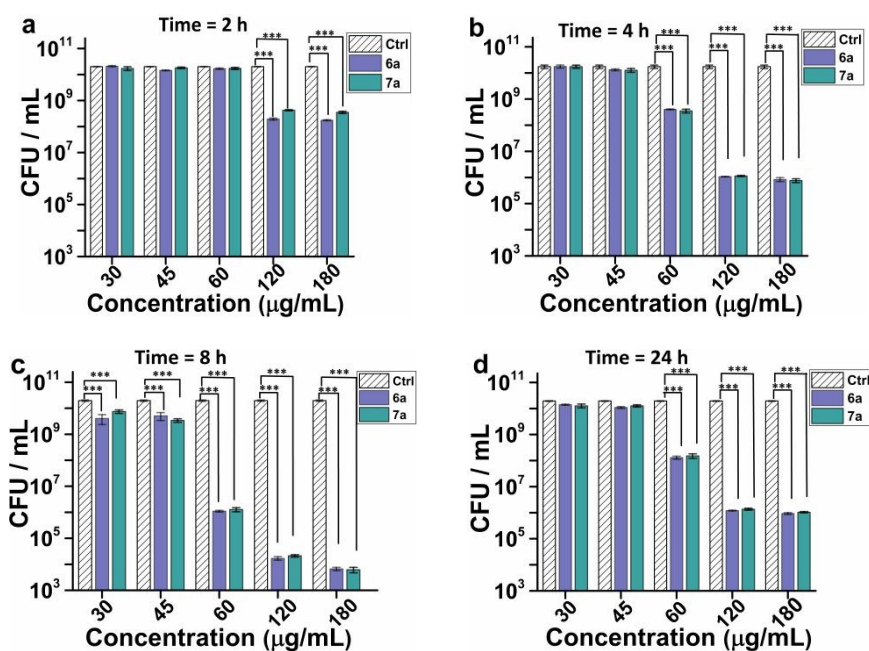


Figure 7. The antimicrobial efficacy of **6a** and **7a** at various concentrations against 48-h-old *S. aureus* biofilm after incubation at 37 °C in the dark for different times (2, 4, 8, 24 h). Data are expressed as means \pm S.D. over three independent experiments; ***P < 0.0001. View Article Online
DOI: 10.1039/D0OB00564A

NO is identified as a key mediator of biofilm dispersal conserved across microbial species³⁴. Subsequently, we carried the experiment with light-irradiation to test the effect of NO on biofilm. UV irradiation could damage the mammalian cells due to the formed reactive oxygen and nitrogen species³⁵, although UV irradiation has been used as a therapeutic agent for various skin diseases³⁶. It was reported that UVA (315-400 nm) induces erythema after 24 h, whereas the erythema develops 4-6 h after the treatment of UVB (280-315 nm)³⁶. Therefore, we set the irradiation time as 4 h to maximize NO release but minimize the potential toxic effect. To rule out any effect of the light irradiation itself on bacterial biofilm, a set of control experiments (PBS) with up to 4 h exposure to light (313 nm) were conducted. Our results showed no light-induced reduction in bacterial biofilm. In the experimental groups, it is

clear that **7a** at a low concentration of 45 $\mu\text{g}/\text{mL}$ still gave a significantly larger reduction in biofilm CFUs (ca. 3-log) at 8 h compared with **6a** (ca. 0.3-log) under light irradiation or **7a** without irradiation (ca. 0.3-log) (Fig. 8). At the concentration of 60 $\mu\text{g}/\text{mL}$, 6-log reduction in CFUs was observed for **7a** at 8 h under irradiation, which is about 2-log reduction than **6a** or non-irradiated **7a**. Taking into account the possibility of the NO formation from **7a** under irradiation, as well as known anti-biofilm activity of a number of NO donors, we can conclude that the enhanced anti-biofilm activity of **7a** under irradiation is due to the combined effect from the photo-generated NO. However, the efficacy difference between the irradiation and non-irradiation group disappeared after 24 h (Fig. 8d). Taken together, **7a** is a “two-in-one” hybrid with good antimicrobial efficacy on *S. aureus* biofilm cells.

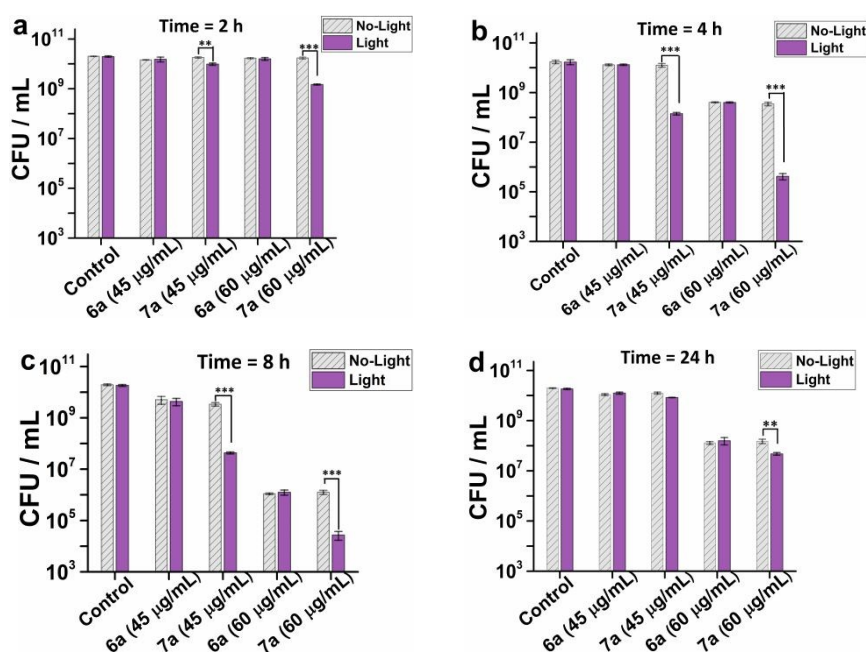


Figure 8. The antibiofilm activities of **7a** (45 and 60 $\mu\text{g}/\text{mL}$) against 48-h-old *S. aureus* biofilm. The biofilm was incubated with **7a** and then exposed to light irradiation (313 nm) for 4 h to allow the NO release. Subsequently, the antibiofilm effect was evaluated at different times (2, 4, 8, 24 h). Data are expressed as means \pm S.D. over three independent experiments; *** p < 0.0001.

It has been reported that QACs and QPCs are able to kill bacteria by damaging cell walls and membrane.²² To investigate structural modifications of *S. aureus* biofilm-detached cells after treatment with **7a** and **6a** in the dark, the morphology of the *S. aureus* bacteria was analyzed by scanning electron microscopy (SEM). As shown in Fig. 9, *S. aureus* biofilm cells looked round in the PBS-treated group and exhibited an undamaged normal smooth lining. After treatment with **7a** or **6a** (60 $\mu\text{g}/\text{mL}$) for 24 h in the dark, the morphology of the bacteria underwent a transformation from their initial round and smooth surfaces to irregular structures. Since NO release from **7a** can be induced by light, we

investigated the combined effect of NO and cationic groups on the morphology of the bacteria. No difference in cell walls was found for the bacteria only exposed to light or in the dark (control and **6a** groups), indicating that the light irradiation has no contribution to bacterial biofilm. In contrast, exposure to light in the presence of **7a** led to more significant damage of the cell walls as compared to the treatment in the dark, supporting that NO and cationic groups have the combined effect on the bacterial biofilm. The change in the morphology of the cell walls was considered to be detrimental to the bacteria, accounting for the antibacterial activity of **7a**.

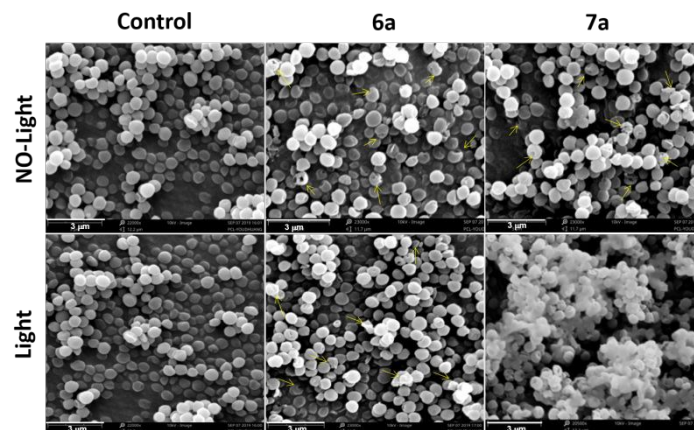


Figure 9. Scanning electron microscope photographs of *S. aureus* biofilm treated with **6a** or **7a** (60 µg/mL) for 24 h after exposure to light for 4 h or in the dark. The control group was treated with sterile PBS in the same condition. Scan bar = 3 µm

In addition, we also assessed the selectivity of the NO hybrids for bacterial over mammalian cell membranes by conducting hemolytic assay on sheep red blood cells. As shown in Fig. S12, very low haemolysis (less than 1%) was observed for all the hybrids (**7a-c**) and their corresponding NO-released products (**6a-b**, **6d**) at the concentration range from 300 to 600 µg/mL. Comparatively, QPCs **7a** and **6a** showed slightly higher haemolysis compared to QACs **7b** and **7c** possibly due to the high hydrophobicity of the TPP group, which facilitated their insertion into the red blood cell membrane. These results indicated that these compounds have high hemocompatibility.

Conclusions

We have designed and synthesized a new type of multifunctional NO hybrids based on benzothienoazepine scaffold and quaternary phosphonium or ammonium. NO release from the NO hybrids is controlled with temporal precision by light irradiation and calibrated by the generated fluorescence from the NO-released product. In addition, light irradiation of the NO hybrids leads to the generation of NO at nearly zero-order release rate and ensures constant release of NO, unlike the previously reported NO donors which have one-order release kinetics. Upon photoactivation, such “two-in-one” hybrids release active gas molecule NO and the conjugates of benzothienoazepine with quaternary phosphonium or ammonium, enabling potent activity against gram-positive bacteria *S. aureus* biofilm. Our work provides a new strategy for design of controllable NO hybrids and new antibacterial compounds.

Conflicts of interest

There are no conflicts to declare.

Acknowledgements

This work was financially supported by the National

Natural Science Foundation of China (No. 81973269, 81603064, 21871210 and 21603163), Science & Technology Projects of Tianjin (18JCYBJC95300 and 18JCQJNC76100), The Open Project Program of Tianjin Key Laboratory on Technologies Enabling Development of Clinical Therapeutics and Diagnostics (Theranostics) and Tianjin Municipal 13th five year plan (Tianjin Medical University Talent Project).

Notes and references

1. C. A. Fux, J. W. Costerton, P. S. Stewart and P. Stoodley, *Survival strategies of infectious biofilms*, *Trends Microbiol*, 2005, **13**, 34-40.
2. D. Davies, *Understanding biofilm resistance to antibacterial agents*, *Nat Rev Drug Discov*, 2003, **2**, 114-122.
3. U. Romling and C. Balsalobre, *Biofilm infections, their resilience to therapy and innovative treatment strategies*, *J Intern Med*, 2012, **272**, 541-561.
4. P. S. Stewart and J. William Costerton, *Antibiotic resistance of bacteria in biofilms*, *The Lancet*, 2001, **358**, 135-138.
5. N. Barraud, B. G. Kardak, N. R. Yepuri, R. P. Howlin, J. S. Webb, S. N. Faust, S. Kjelleberg, S. A. Rice and M. J. Kelso, *Cephalosporin-3'-diazoniumdiolates: targeted NO-donor prodrugs for dispersing bacterial biofilms*, *Angew Chem Int Ed Engl*, 2012, **51**, 9057-9060.
6. D. P. Arora, S. Hossain, Y. Xu and E. M. Boon, *Nitric Oxide Regulation of Bacterial Biofilms*, *Biochemistry*, 2015, **54**, 3717-3728.
7. J. Zaitseva, V. Granik, A. Belik, O. Koksharova and I. Khmel, *Effect of nitrofurans and NO generators on biofilm formation by Pseudomonas aeruginosa PAO1 and Burkholderia cenocepacia 370*, *Res Microbiol*, 2009, **160**, 353-357.
8. D. McDougald, S. A. Rice, N. Barraud, P. D. Steinberg and S. Kjelleberg, *Should we stay or should we go: mechanisms and ecological consequences for biofilm dispersal*, *Nat Rev Microbiol*, 2011, **10**, 39-50.
9. S. Hossain, L. M. Nisbett and E. M. Boon, *Discovery of Two Bacterial Nitric Oxide-Responsive Proteins and Their Roles in Bacterial Biofilm Regulation*, *Acc Chem Res*, 2017, **50**, 1633-1639.
10. R. P. Howlin, K. Cathie, L. Hall-Stoodley, V. Cornelius, C. Duignan, R. N. Allan, B. O. Fernandez, N. Barraud, K. D. Bruce, J. Jefferies, M. Kelso, S. Kjelleberg, S. A. Rice, G. B. Rogers, S. Pink, C. Smith, P. S. Sukhtankar, R. Salib,

- J. Legg, M. Carroll, T. Daniels, M. Feelisch, P. Stoodley, S. C. Clarke, G. Connett, S. N. Faust and J. S. Webb, *Low-Dose Nitric Oxide as Targeted Antibiofilm Adjunctive Therapy to Treat Chronic Pseudomonas aeruginosa Infection in Cystic Fibrosis*, *Mol Ther*, 2017, **25**, 2104-2116.
11. S. K. Kutty, N. Barraud, A. Pham, G. Iskander, S. A. Rice, D. S. Black and N. Kumar, *Design, synthesis, and evaluation of fimbrolide-nitric oxide donor hybrids as antimicrobial agents*, *J Med Chem*, 2013, **56**, 9517-9529.
12. N. R. Yepuri, N. Barraud, N. S. Mohammadi, B. G. Kardak, S. Kjelleberg, S. A. Rice and M. J. Kelso, *Synthesis of cephalosporin-3'-diazoniumdiolates: biofilm dispersing NO-donor prodrugs activated by beta-lactamase*, *Chem Commun* 2013, **49**, 4791-4793.
13. Z. Sadrearhami, T.-K. Nguyen, R. Namivandi-Zangeneh, K. Jung, E. H. H. Wong and C. Boyer, *Recent advances in nitric oxide delivery for antimicrobial applications using polymer-based systems*, *J Mater Chem B*, 2018, **6**, 2945-2959.
14. A. Rineh, O. Soren, T. McEwan, V. Ravikumar, W. H. Roh, F. Azamifa, M. R. Naimi-Jamal, C.-Y. Cheung, A. G. Elliott, J. Zuegg, M. A. T. Blaskovich, M. A. Copper, V. Dolange, M. Christodoulides, G. M. Cook, S. A. Rice, S. N. Faust, J. S. Webb M. J. Kelso, *Discovery of Cephalosporin-3'-Diazoniumdiolates That Show Dual Antibacterial and Antibiofilm Effects against Pseudomonas aeruginosa Clinical Cystic Fibrosis Isolates and Efficacy in a Murine Respiratory Infection Model*, *ACS Infect. Dis.*, 2020, doi: 10.1021/acscinfecdis.0c00070
15. M. Guo, H. J. Xiang, Y. Wang, Q. L. Zhang, L. An, S. P. Yang, Y. Ma, Y. Wang and J. G. Liu, *Ruthenium nitrosyl functionalized graphene quantum dots as an efficient nanoplatform for NIR-light-controlled and mitochondria-targeted delivery of nitric oxide combined with photothermal therapy*, *Chem Commun*, 2017, **53**, 3253-3256.
16. K. Hishikawa, H. Nakagawa, T. Furuta, K. Fukuhara, H. Tsumoto, T. Suzuki and N. Miyata, *Photoinduced Nitric Oxide Release from a Hindered Nitrobenzene Derivative by Two-Photon Excitation*, *J Am Chem Soc*, 2009, **131**, 7488-7489.
17. S. Namiki, T. Arai and K. Fujimori, *High-Performance Caged Nitric Oxide: A New Molecular Design, Synthesis, and Photochemical Reaction*, *J Am Chem Soc*, 1997, **119**, 3840-3841.
18. E. Y. Zhou, H. J. Knox, C. J. Reinhardt, G. Partipilo, M. J. Nilges and J. Chan, *Near-Infrared Photoactivatable Nitric Oxide Donors with Integrated Photoacoustic Monitoring*, *J Am Chem Soc*, 2018, **140**, 11686-11697.
19. H. He, Y. Liu, Z. Zhou, C. Guo, H. Y. Wang, Z. Wang, X. Wang, Z. Zhang, F. G. Wu, H. Wang, D. Chen, D. Yang, X. Liang, J. Chen, S. Zhou, X. Liang, X. Qian and Y. Yang, *A Photo-triggered and photo-calibrated nitric oxide donor: Rational design, spectral characterizations, and biological applications*, *Free Radic Biol Med*, 2018, **123**, 1-7.
20. J. P. Cheng, M. Xian, K. Wang, X. Zhu, Z. Yin and P. G. Wang, *Heterolytic and Homolytic Y-NO Bond Energy Scales of Nitroso-Containing Compounds: Chemical Origin of NO Release and NO Capture*, *J Am Chem Soc*, 1998, **120**, 10266-10267.
21. E. A. F. Fordyce, D. W. Brookes, C. Lise-Ciana, M. S. Coates, S. F. Hunt, K. Ito, J. King-Underwood, S. T. Onions, G. F. Parra, G. Rapeport, V. Sherbukhin, J. A. Stockwell, P. Strong, J. C. Thomas and J. Murray, *Discovery of novel benzothienoazepine derivatives as potent inhibitors of respiratory syncytial virus*, *Bioorg Med Chem Lett*, 2017, **27**, 2201-2206.
22. A. Muñoz-Bonilla and M. Fernández-García, *Polymeric materials with antimicrobial activity*, *Prog Polym Sci*, 2012, **37**, 281-339.
23. A. Y. Shirashi M, Seto M, Imoto H, Nishikawa Y, Kanzaki N, Okamoto M, Sawada H, Nishimura O, Baba M, Fujino M, *Discovery of Novel, Potent, and Selective Small-Molecule CCR5 Antagonists as Anti-HIV-1 Agents: Synthesis and Biological Evaluation of Anilide Derivatives with a Quaternary Ammonium Moiety*, *J Med Chem*, 2000, **43**, 2049-2063. DOI: 10.1039/D00B00564A
24. V. Peesapati and N. Lingaiah, *Thiopheno[3,2][1]benzazepine, benzo[3,4]cyclohepta[2,1-b]thiophenes, thiazolo[5,4-d][1]benzazepine and benzo[3,4]cyclohepta[2,1-d]thiazoles*, *Org Prep Proced Int*, 1993, **25**, 602-606.
25. Z. Zhang, J. Wu, Z. Shang, C. Wang, J. Cheng, X. Qian, Y. Xiao, Z. Xu and Y. Yang, *Photocalibrated NO Release from N-Nitrosated Naphthalimides upon One-Photon or Two-Photon Irradiation*, *Anal Chem*, 2016, **88**, 7274-7280.
26. Y. Duan, Y. Wang, X. Li, G. Zhang, G. Zhang and J. Hu, *Light-triggered nitric oxide (NO) release from photoresponsive polymersomes for corneal wound healing*, *Chem Sci*, 2020, **11**, 186-194.
27. A. Ramamurthi and R. S. Lewis, *Measurement and modeling of nitric oxide release rates for nitric oxide donors*, *Chem Res Toxicol*, 1997, **10**, 408-413.
28. Y. Kotake, T. Tanigawa, M. Tanigawa, I. Ueno, D. R. Allen and C. S. Lai, *Continuous monitoring of cellular nitric oxide generation by spin trapping with an iron-dithiocarbamate complex*, *Biochim Biophys Acta*, 1996, **1289**, 362-368.
29. J. S. Wishnok, J. A. Glogowski and S. R. Tannenbaum, *Quantitation of Nitrate, Nitrite, and Nitrosating Agents*, *Methods Enzymol.*, 1996, **268**, 130-141.
30. S. Garcia-Arguelles, M. C. Serrano, M. C. Gutierrez, M. L. Ferrer, L. Yuste, F. Rojo and F. del Monte, *Deep eutectic solvent-assisted synthesis of biodegradable polyesters with antibacterial properties*, *Langmuir*, 2013, **29**, 9525-9534.
31. T. J. Cuthbert, B. Hisey, T. D. Harrison, J. F. Trant, E. R. Gillies and P. J. Ragona, *Surprising Antibacterial Activity and Selectivity of Hydrophilic Polyphosphoniums Featuring Sugar and Hydroxyl Substituents.pdf*, *Angew Chem Int Ed Engl*, **57**, 12707-12710.
32. M. R. Parsek and P. K. Singh, *Bacterial biofilms: an emerging link to disease pathogenesis*, *Annu Rev Microbiol*, 2003, **57**, 677-701.
33. S. Kumar Shukla and T. S. Rao, *Dispersal of Bap-mediated Staphylococcus aureus biofilm by proteinase K*, *J Antibiot (Tokyo)*, 2013, **66**, 55-60.
34. N. Barraud, M. J. Kelso, S. A. Rice and S. Kjelleberg, *Nitric oxide: a key mediator of biofilm dispersal with applications in infectious diseases*, *Curr Pharm Des*, 2015, **21**, 31-42.
35. T. J. McMillan, E. Leatherman, A. Ridley, J. Shorrocks, S. E. Tobi, J. R. Whiteside, *Cellular Effects of Long Wavelength UV Light (UVA) in Mammalian Cells*, *J Pharm Pharmacol*, 2008, **60**, 969-976.
36. Y. Matsumura, H. N. Anathaswamy, *Toxic Effects of Ultraviolet Radiation on the Skin*, *Toxicol Appl Pharmacol*, 2004, **195**, 298-308